Indian Journal of Fibre & Textile Research
Vol. 41, March 2016, pp. 13-18

Morphological and thermal properties of optimized electrospun cellulose acetate nanofibres during deacetylation in different *p*H values

Payam Zahedi[1,a] , Ayda Rafie[1] & Edyta Wojczak[2]

[1]School of Chemical Engineering, College of Engineering, University of Tehran, PO Box 11155-4563 Tehran, Iran

[2] Institute of Applied Radiation Chemistry, Technical University, Wróblewskiego 15, 93-590 Lodz, Poland

Received 11 August 2014; revised received and accepted 3 December 2014

The aim of this study is to investigate morphology, molecular structure and thermal behavior of optimized cellulose acetate nanofibrous mats during deacetylation reaction in both basic and acidic environments. Firstly, the polymer concentration, applied voltage, flow rate and syringe needle tip-collector distance have been optimized via a response surface methodology. This optimization of the above independent variables leads to obtain a uniform and smooth morphology for cellulose acetate nanofibrous samples with a minimum average diameter of 166.2 nm. Afterward, the effect of basic and acidic environments on the morphologies, functional groups changes on the surface of the samples and their thermal behaviors have been studied by using scanning electron microscopy (SEM), Fourier transformed infra-red (FTIR)spectroscopy and differential scanning calorimetry (DSC) respectively. The FTIR results show that a deacetylation reaction occurs in nanofibrous samples treated with KOH solution as compared to those samples treated with HCl solution. Due to the altering functional groups in the chemical structure, cellulose acetate nanofibres are converted to cellulose with a semi-film like shape. The SEM micrographs confirm these results obtained from FTIR spectra. DSC thermograms reveal different values at melting point of the samples before and after immersion of the samples into the both environments. Moreover, some changes in crystallization appear within the molecular structure of the samples during solidification.

Keywords: Cellulose acetate, Electrospinning, Nanofibres, Thermal behavior

1 Introduction

Cellulose and its derivatives are biodegradable polymers and are renewable resources. Nowadays, using this class of polymers especially in the shape of nanofibrous mats has attracted a great deal of attention due to their high surface-to-volume or length-to-diameter ratios. These characteristics are essential for practical applications such as separation membranes, wound dressing materials, sensors, composite reinforcements, biomedical applications, etc.[1-3].

Electrospinning is a method in order to produce nanofibres formed by subjecting a high-viscosity polymer solution to a high electric field[4-6]. It is an abundant process for creation of the ultrafine fibres from polymer melt or solution because of the simplicity, high efficiency and cost effectivity of this technique compared to other methods for providing the nanofibrous mats[7]. The morphology of as-spun nanofibres is governed by the following two conditions namely (i) the polymer material characteristics such as molecular weight, molecular weight distribution and structure (branched and linear) and the polymer solution characteristics (viscosity and solvent type); and (ii) the electrospinning parameters in terms of applied voltage, distance between the syringe needle tip and the collector, and solution flow rate. In our previous work[8], we optimized the above parameters for the production of electrospun poly (vinyl alcohol)/poly (*ε*-caprolactone) (PVA/PCL) hybrid nanofibres via D-optimal design method. The results showed that for providing the samples with a minimum average diameter of about 220 nm for PVA along with a uniform and smooth morphology, the electrospinning variables should be determined as follows: flow rate (0.8 mL/h), the distance between the needle tip and the collector (10 cm) and applied voltage (19.5 kV). Subsequently, this trend was also used to produce the similar morphology for PCL via electrospinning.

Although solvents for cellulose are not completely volatile and require coagulation steps to ensure complete removal of the solvent from electrospun fibres, the tendency is to use some cellulose

[a]Corresponding author.
E-mail: phdzahedi@ut.ac.ir

derivatives i.e. cellulose acetate (CA). Cellulose acetate, in particular, has been electrospun using a wide variety of volatile solvents. Also, its nanofibres can be converted to cellulose nanofibres by using deacetylation reaction. Some research works have been carried out for the development of a suitable solvents mixture[9,10] as well as optimization of electrospinning parameters for minimizing average diameter of CA nanofibrous samples[11]. Nista *et al.*[12] investigated the best solvents and electrospinning conditions for nanostructured membranes based on CA. They successfully prepared nanofibres via electrospinning in the presence of four mixed solvents, viz acetic acid/water, acetone/water, dimethylacetamide (DMAc)/acetone and DMAc/ acetone/water. Moreover, the as-spun nanofibres in these different solvents mixtures were optimized by design of experiments (DOE). For example, they considered three variables such as CA concentration, potential and needle-collector distance for acetic acid: water (3: 1 w/w) mixture in order to achieve ultrafine CA fibres. The following conditions were used for CA nanofibres with an average diameter of 180±60 nm: CA concentration 17 (%w/w), potential 15 kV and needle-collector distance 10 cm.

In other studies[13,14], a few works have been done to study the effect of deacetylation of ultrafine CA fibres in different acidic and basic environments. In an interesting research work, Han *et al.*[15] analyzed the changes in chemical structure of CA nanofibres during deacetylation by using FTIR spectroscopy. Their results reveal that two main characteristic peaks for CA corresponding to C–O and C–O–C groups at 1745 cm^{-1} and 1235 cm^{-1} respectively were disappeared after 30 min of immersion into potassium hydroxide (0.5 N). It can be concluded that during deacetylation reaction, cellulose acetate nanofibres are converted into cellulose nanofibrous samples.

In the above reported literature, the optimization of whole electrospinning parameters using response surface methodology (RSM) for producing ultrafine CA fibres has not been carried out. Additionally, the effect of deacetylation on morphology and thermal behavior of these samples in both acidic (HCl) and basic (KOH) has not been studied in detail.

This study was therefore aimed at designing a general governed equation in order to estimate the ultrafine electrospun CA fibres diameter in accordance with four main parameters in terms of CA concentration, flow rate, applied voltage and the distance between the syringe needle tip and the collector for electrospinning process. Afterward, the morphology and thermal analyses along with the occurred changes in functional groups within the chemical structure of optimized CA nanofibrous samples in both low and high *p*Hs are investigated and discussed.

2 Materials and Methods

2.1 Materials

Cellulose acetate (biodegradable, acetyl content 39.8%, molecular weight 30 kDa) was obtained from Sigma-Aldrich Co., Pillsburg, The Netherlands. Glacial acetic acid (>99.99) was purchased from Merck, Germany. Glacial acetic acid and deionized water were mixed by volume. The mixed solvents containing acetic acid/water (75/25 by volume) was used. The other chemicals were used without further purification.

2.2 D-optimal Design

The experimental plan was carried out by using Design Expert V.6 (Stat-Easy Inc., Minneapolis, MN). Table 1 shows the experimental design made by using

Table 1—D-optimal experimental design

Run	CA concentration % w/v (X_1)	Voltage kV (X_2)	Flow rate mL/h (X_3)	Distance cm (X_4)	Diameter nm (Y)
1	11	20	0.4	18	1369.6
2	19	25	0.7	18	466.7
3	19	15	0.4	18	426
4	19	20	0.7	14	465.4
5	15	15	1	18	1200
6	11	25	0.4	10	1374.8
7	15	15	0.4	10	387.7
8	11	15	1	10	1880.7
9	11	15	1	10	1910.3
10	19	25	1	14	441.6
11	11	25	0.4	10	1373.4
12	19	25	0.4	10	430.3
13	19	20	1	18	374.6
14	11	25	1	18	2066
15	15	25	0.4	18	1250
16	19	25	0.4	10	422.6
17	11	15	0.7	18	3006.7
18	13	20	0.7	14	3434.7
19	11	25	1	18	2098.7
20	15	25	1	10	1300
21	19	15	1	10	286.2
22	11	15	0.4	14	3500
23	19	15	1	10	281.7

D-optimal in 23 runs to observe the diameter of CA nanofibres. As it can be seen from this table, four different independent parameters, viz CA concentration, applied voltage, flow rate and distance between the needle tip and the collector are represented by X_1, X_2, X_3 and X_4 respectively. On this basis, the effects of all the parameters (X_1-X_4) on the answer (Y_1) were investigated. Finally, in response, a polynomial model based on these effective parameters and their interactions is fixed and demonstrated as a generalized scheme.

2.3 Electrospinning

Weighed CA powder was completely dissolved in mixed acetic acid/water (75/25) and then various CA concentrations from 11 to 19 (%w/v) were prepared. The electrospinning device used for the preparation of samples was eSpinner NF-COEN/II of Asian Nanostructures Technology Co., Iran. The electrospinning conditions for CA samples were: solution flow rate 1 mL/h, voltage 19.5 kV, gauge needle 0.7 mm and distance between the needle tip and the rotational collector 10 cm. The as-spun CA fibres were collected on a sterilized foil. To achieve fully dried electrospun nanofibrous samples and to ensure evaporation of the organic solvents from the spun fibres, the samples were then dried at room temperature for about 12 h until a constant weight was attained.

2.4 SEM Studies

Electrospun nanofibres on aluminum foil were coated with a thin layer of gold by a Bio-Rad E5200 auto sputter coater (England). For the morphological observations of the samples a scanning electron microscopy (AIS 2100 model, Seron Technologies Inc., Korea) with ×10000 magnification was used. The mean values of the nanofibres diameters from ten different sections were measured by ImageJ software and recorded. The standard deviation was calculated as <5%.

2.5 FTIR Studies

Due to investigation of some changes in functional groups within the chemical structure of CA nanofibrous samples before and after immersing into KOH and HCl (0.5 N) solutions for 3 h, an attenuated total reflectance-Fourier transformed infrared (ATR-FTIR) spectroscopy (model EQUINOX 55, Bruker Co., United States) was used. The wavenumber range used in FTIR spectroscopy was 600-4000 cm^{-1}.

2.6 Thermal Analysis of Samples

Differential scanning calorimetry (DSC) analysis of electrospun CA nanofibrous mats with and without treatment in different pHs was carried out on a DSC-OIT (model DSC 400, Sanaf Co., Iran) at a heating rate of 10°C/min. Before DSC analysis, all the samples were fully dried in a vacuum chamber at 40°C for 24 h and kept in a desiccator containing silica gel. Then, the electrospun samples were sealed in aluminum pans and heated from room temperature to 350°C.

3 Results and Discussion

3.1 Optimized CA Nanofibrous Samples via D-optimal Design

D-optimal design is a powerful and precise technique to optimize a process requiring three or more independent parameters. In this work, four main variables, such as CA concentration (X_1), applied voltage (X_2), flow rate (X_3) and the distance between the syringe needle tip and the collector (X_4) were optimized in order to obtain a minimum average diameter (Y) for CA nanofibrous samples. After analyzing the data, a generalized quadratic equation for calculating Y against each X by D-optimal design was achieved. Following equation shows the relationships between main variables and their interactions with respect to the response (Y):

$$Y = -2434.8 - 404.8X_1 - 417.9X_2 + 8090.7X_3 + 1552.8X_4 + 3.7X_1X_2 - 75.2X_1X_3 + 10.6X_1X_4 - 5.6X_2X_4 + 10.1X_2^2 - 4954.6X_3^2 - 56X_4^2 \quad ,\ldots(1)$$

The best amounts of each effective parameter along with the response (Y) for the electrospinning conditions are CA concentration (X_1) 17 (% w/v), applied voltage (X_2) 19.5 kV, flow rate (X_3) 1 mL/h, and distance between the needle tip and the collector (X_4) 10 cm.

According to the above conditions, the minimum average diameter of CA nanofibres was about 166.2 nm. The regression coefficient (r^2) for Eq. (1) was estimated to be 0.95. Figures 1 (a)-(d) exhibit the interactions between some effective parameters and CA nanofibres average diameter variations. As it can be observed from Figs 1 (a)-(c), CA concentration parameter has a linear and non-proportional relation with respect to the CA average diameter in the presence of the voltage, flow rate and distance at their constant values. Figure 1 (d) demonstrates that the voltage variable has a non-linear behavior against

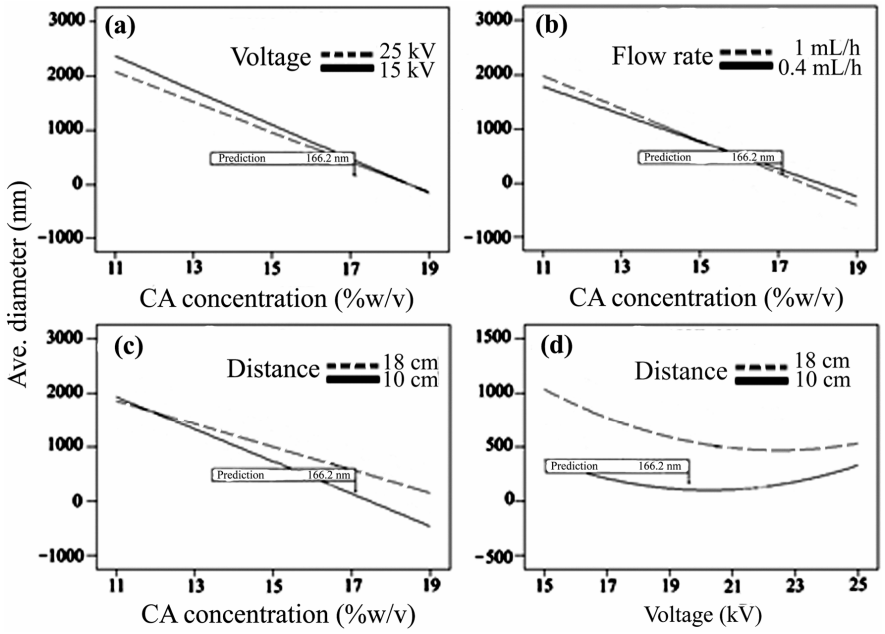

Fig. 1—Variations in average diameter of cellulose acetate nanofibrous samples with effective independent factors and their interactions

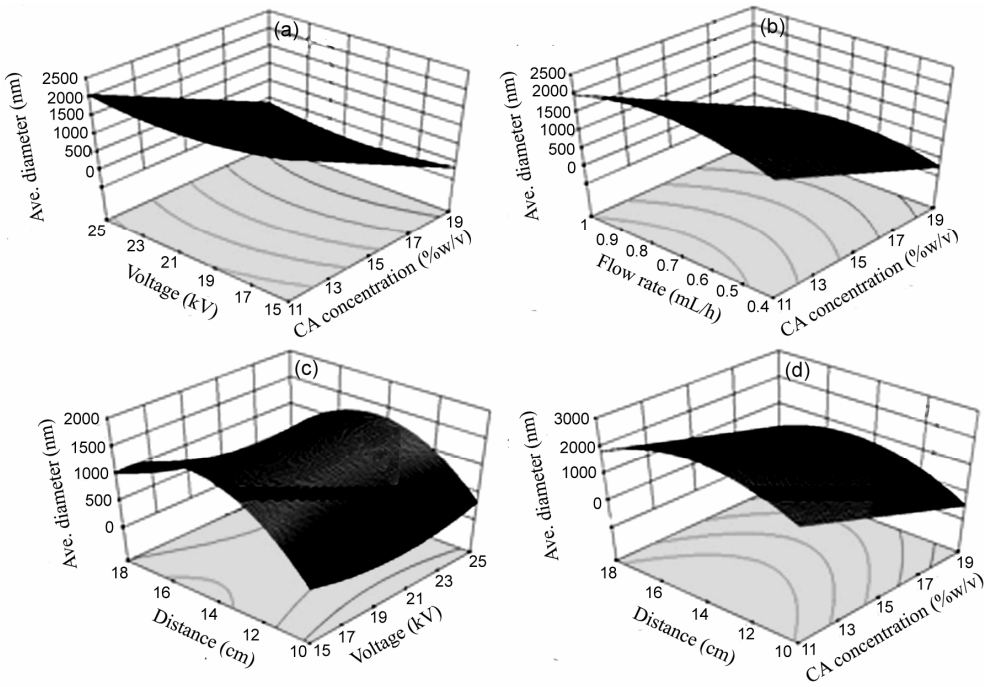

Fig. 2—Three-dimensional graphs of the nanofibres average diameter as surface response results against (a) voltage and CA concentration, (b) flow rate and CA concentration, (c) needle-collector distance and voltage and (d) needle-collector distance and CA concentration

the average diameter in high and low distance parameter. This trend appears at an optimized point for voltage (19.5 kV). A little increase or decrease of this specific point causes a remarkable raising in the nanofibres average diameter. Figures 2 (a)-(d) give a more vision for the relationship between the whole important parameters against CA nanofibres average diameter. These 3-dimensional graphs show that a curvature behavior is governed by the trends among four parameters, such as voltage, CA concentration, flow rate and the needle-collector distance with respect to the CA nanofibres average diameter.

3.2 Effect of *p*Hs on Changes in Chemical Structure of CA Nanofibres

Table 2 shows the peak frequencies of FTIR spectra for three optimized CA nanofibrous samples under different environmental conditions. The characteristic peaks for CA nanofibres without treatment against acidic or basic environments, correspond to C–O group at 1736.12 cm^{-1} and C–O–C group at 1219.69 cm^{-1}. To investigate the effect of high and low *p*Hs on changes in chemical structure of CA nanofibres, they were immersed into KOH and HCl (0.5 N) environments for 3 h. The resulting FTIR spectra of the sample at the exposure of KOH show that the two main characteristic peaks (C–O and C–O–C groups) as explained before completely disappear. This phenomenon indicates occurrence of deacetylation reaction as long as the whole acetyl groups are eliminated by KOH and consequently CA nanofibres are converted to cellulose. Due to the substitution of acetyl groups by hydrogen, a remarkable peak at 3202.68 cm^{-1}corresponding to –OH groups is observed. In contrast, FTIR spectrum of CA nanofibres treated with HCl (0.5 N) results in no significant changes in chemical structure of CA nanofibrous samples. This time, the two main characteristic peaks for CA nanofibres appear at 1734.90 cm^{-1} ($\upsilon_{C–O}$) and 1225.70 cm^{-1} ($\upsilon_{C–O–C}$). It can be concluded that from Table 2, HCl solution has no effective interaction on the chemical structure of CA nanofibres. This may be due to the inherent acidic functionalized groups (acetyl) in the molecular structure which causes no changes in the degradation of acetyl groups. In other words, CA nanofibres has a good compatibility with HCl solution as an acidic environment. On the other hand, owing to increase in protons within environment, –OH groups are activated and the characteristic peak of this specific group is highlighted.

3.3 Morphology of Samples

SEM images of optimized CA nanofibrous samples not only confirm the uniformity and smoothness of the ultrafine CA fibres after optimization [Fig. 3 (a)], but also they show that some expected changes occur in the structure of nanofibres when they are immersed into the KOH and HCl environments. As it can be seen from Fig. 3 (b), the CA nanofibres completely form a semi-film like shape. This may due to the effect of KOH solution on the chemical structure of CA followed by deacetylation reaction during 3 h immersion. However, no significant changes appear in the morphology of CA nanofibrous samples when they are immersed into HCl (0.5 N). The above obtained results from SEM images emphasize again the remarkable changes in the chemical structure of CA nanofibres during deacetylation.

Table 2—Significant FTIR peaks for untreated and treated optimized CA nanofibres

Sample	$\upsilon_{C–O}$ cm^{-1}	$\upsilon_{C–O–C}$ cm^{-1}	$\upsilon_{O–H}$ cm^{-1}
Untreated CA	1736.12	1219.69	–
CA treated with HCl	1734.90	1225.70	3379.56
CA treated with KOH	–	–	3202.68

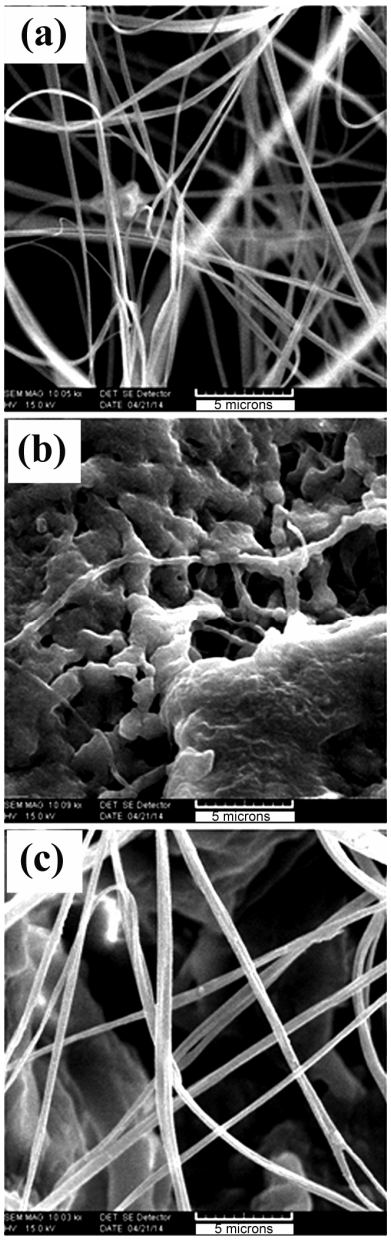

Fig. 3—SEM images of optimized cellulose acetate nanofibrous samples (a) untreated, (b) treated with KOH and (c) treated with HCl (scale bar = 5 microns)

3.4 Thermal Analysis of Optimized CA Nanofibrous Samples

These appear some fundamental changes in thermal behavior of CA nanofibres when they are immersed into acidic and/or basic environments. For this purpose, a differential scanning calorimetry (DSC) study for three different CA nanofibrous samples was carried out. Figure 4 exhibits the DSC thermograms of these samples. As it is evident, a small recrystallization peak at about 50°C is observed for CA nanofibrous sample without treatment. Also, the conventional melting point for this sample is found to be at about 350°C. Nevertheless, a different thermal behavior is considered by the other two samples immersed into KOH and HCl solutions for 3 h. The DSC thermogram of KOH treated sample shows two close peaks related to recrystallization and melting point at 190°C and 250°C respectively. When CA nanofibres are transformed into cellulose nanofibres owing to deacetylation, the crystallization is increased because of the alternation in the chemical structure of the polymer and subsequently, the thermal stability of the samples decreases. Moreover, acetyl groups in the chemical structure of CA nanofibres have a large molecular structure compared to hydroxyl groups in cellulose nanofibres. It causes some restrictions in segmental motions of CA chains and leads to lamellae formation and in consequence, the crystallization capability is increased in CA nanofibres compared to cellulose[16]. Further, the thermogram of CA nanofibrous sample treated with HCl has a similar trend as compared to that of the sample without acid treatment. It should be noted that a little change occurs in the crystallization peak for this sample at temperature of about 70°C due to the increase in hydroxyl groups and this leads to lamellae formation without any significant changes in the amount of acetyl groups.

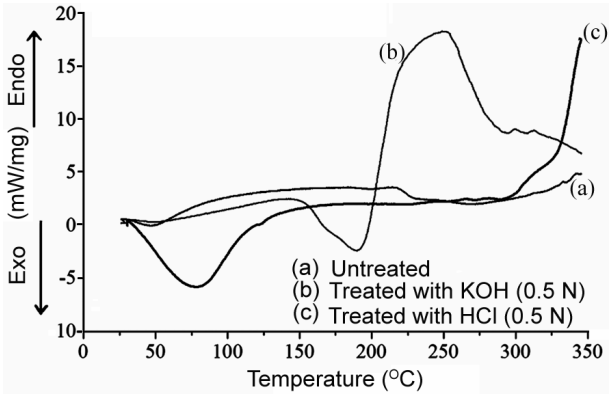

Fig. 4—DSC thermograms of the optimized electrospun cellulose acetate nanofibrous samples

4 Conclusion

We have successfully optimized the electrospinning parameters for minimizing average diameter of cellulose acetate nanofibres via D-optimal design. For this purpose, the independent variables are calculated as CA concentration 17 (%w/v), solution flow rate 1 mL/h, distance between the syringe needle tip and the collector 10 cm and, applied voltage 19.5 kV. These optimized inputs for the variables lead to produce CA nanofibres with average diameter of about 166.2 nm. Afterward, the prepared and optimized samples are immersed into the KOH and HCl environments for investigating their morphologies and thermal behavior. The results show that a high *p*H value is capable to completely change the chemical structure of CA nanofibrous samples and convert them to cellulose. Also, the optimized samples treated with KOH solution demonstrate a remarkable shifts in DSC thermograms at recrystallization and melting point temperatures as compared to those treated with HCl. Finally, it can be concluded that the entire phenomena occur due to deacetylation reaction in cellulose acetate nanofibres.

References

1 Frey M W, *Polym Rev,* 48 (2008) 378.
2 Ma Z, Kotaki M & Ramakrishna S, *J Membrane Sci,* 265 (2005) 115.
3 Kim C W, Kim D S, Kang S Y, Marquez M & Yoo Y L, *Polymer*, 47 (2006) 5097.
4 Shin Y M, Hohman M M, Brenner M P & Rutledge G C, *Polymer*, 42 (2001) 9955.
5 Deitzel J M, Kosik W, McKnight S H, Beck Tan N C, DeSimmone J M & Crette S, *Polymer*, 43 (2002) 1025.
6 Ramakrishna S, Fujihara K, Teo W E, Yong T, Ma Z & Ramaseshan R, *Mater Today*, 9 (2006) 40.
7 Zahedi P, Rezaeian I, Ranaei-Siadat S O, Jafari S H & Supaphol P, *Polym Adv Technol*, 21 (2010) 77.
8 Zahedi P, Rezaeian I, Jafari S H & Karami Z, *Macromol Res*, 21 (2013) 649.
9 Tungprapa S, Puangparn T, Weerasombut M, Jangchud I, Fakum P, Semongkhol S, Meechaisue C & Supaphol P, *Cellulose*, 14 (2007) 563.
10 Haas D, Heinrich S &Greil P, *J Mater Sci*, 45 (2010) 1299.
11 Konwarh R, Misra M, Mohanty A K & Karak N, *Carbohyd Polym*, 92 (2013) 1100.
12 Nista S V G, Peres L, D´Ávila M A, Schmidt F L & Mei L H I, *J Appl Polym Sci*, 126 (2012) 70.
13 Khatri Z, Wei K, Kim B S & Kim I S, *Carbohyd Polym*, 87 (2012) 2183.
14 Son W K, Youk J H, Lee T S & Park W H, *J Polym Sci Part B Polym Phys*, 42 (2004) 5.
15 Han S O, Youk J H, Min K D, Kang Y O & Park W H, *Mater Lett*, 62 (2008) 759.
16 Barud H S, dA Júnior A M, Santos D B, dAssuncao R M N, Meireles C S, Cerqueira D A, Filho G R, Ribeiro C A, Messaddeq Y& Ribeiro S J L, *Thermochim Acta,*471 (2008) 61.